JOC Article
pubs.acs.org/joc

Theoretical Study of 1,6-Anhydrosugar Formation from Phenyl D-Glucosides under Basic Condition: Reasons for Higher Reactivity of β-Anomer

Takashi Hosoya,[†] Yoshihide Nakao,[‡] Hirofumi Sato,[‡] and Shigeyoshi Sakaki*[,§]

[†]*Department of Chemistry, Graduate School of Science, Kyoto University, Kitashirakawa-oiwaketyo, Sakyo-ku, Kyoto 606-8502, Japan,* [‡]*Department of Molecular Engineering, Graduate School of Engineering, Kyoto University, Kyotodaigaku-katsura, Nishikyo-ku, Kyoto 615-8510, Japan, and* [§]*Institute for Integrated Cell-Material Sciences, Kyoto University, Yoshida-ushinomiya-cho, Sakyo-ku, Kyoto 606-8501, Japan*

sakaki@moleng.kyoto-u.ac.jp

Received August 10, 2010

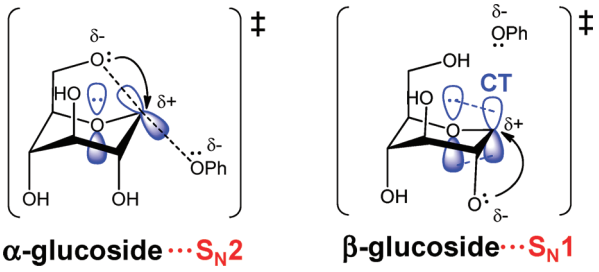

Degradation of anomeric phenyl D-glucosides to levoglucosan under basic condition is theoretically studied. MP4(SDQ)//DFT(B3LYP)-computational results indicate that the degradation of phenyl α-glucoside ($\mathbf{R_\alpha}$) occurs via the $S_N$icB mechanism. In this mechanism, the oxyanion at the C6, which is formed through deprotonation of the OH group, directly attacks the anomeric carbon. On the other hand, the degradation of phenyl β-glucoside ($\mathbf{R_\beta}$) occurs via the $S_N$icB(2) mechanism. In this mechanism, the oxyanion at the C2 attacks the anomeric carbon in a nucleophilic manner to afford 1,2-anhydride intermediate and then the oxyanion at the C6 attacks the anomeric carbon to afford levoglucosan. The activation barrier is much lower in the reaction of $\mathbf{R_\beta}$ ($\Delta G^{0‡}$ = 25.6 kcal/mol and E_a = 26.5 kcal/mol) than in the reaction of $\mathbf{R_\alpha}$ ($\Delta G^{0‡}$ = 38.1 kcal/mol and E_a = 37.2 kcal/mol), which is consistent with the experimental observation that β-glucoside is generally much more reactive than the corresponding α-glucoside. The lower activation barrier of the reaction of $\mathbf{R_\beta}$ arises from the stereoelectronic effect, which is induced by the charge transfer from the ring oxygen to the anomeric carbon, and the staggered conformation around the C1−C2 bond. When the stereoelectronic effect is absent, the degradation needs larger activation energy; for instance, the degradation of phenyl 5a-carba-β-D-glucoside ($\mathbf{R_{C\beta}}$) occurs with large $\Delta G^{0‡}$ and E_a values like those of α-glucosides, because the methylene group of $\mathbf{R_{C\beta}}$ does not contribute to the stereoelectronic effect. Also, the conformation around the C1−C2 bond is staggered in the transition state of the $\mathbf{R_\beta}$ reaction but eclipsed in that of the $\mathbf{R_\alpha}$ reaction, which also leads to the larger reactivity of $\mathbf{R_\beta}$.

1. Introduction

Degradation of glycosides occurs via cleavage of their glycosidic bonds under basic condition.[1−16] In this degradation, such glycosides as glucosides and galactosides produce a considerable amount of the corresponding 1,6-anhydrosugars.[1−9,13,15,16] This degradation is one of the key steps in the syntheses of various glycosides and polysaccharides, because 1,6-anhydrosugars are employed as glycosyl donors in those syntheses.[17−19] Also, the degradations of such β-glycans as cellulose, glucomannan, and xylan, which are major wood components, are very industrially important, because these degradations are believed to induce undesirable depolymerization of carbohydrates in the pulp-making process.[3−5]

The $S_N$icB(2) mechanism was previously proposed for the formation of levoglucosan (1,6-anhydro-β-D-glucopyranose) from β-glucoside under basic condition,[4−9] as shown in Scheme 1A. This mechanism involves two steps of intramolecular nucleophilic substitution at the anomeric carbon:

Published on Web 11/17/2010 DOI: 10.1021/jo101494g

SCHEME 1. Levoglucosan Formation from α- and β-Phenyl Glucosides under Basic Condition

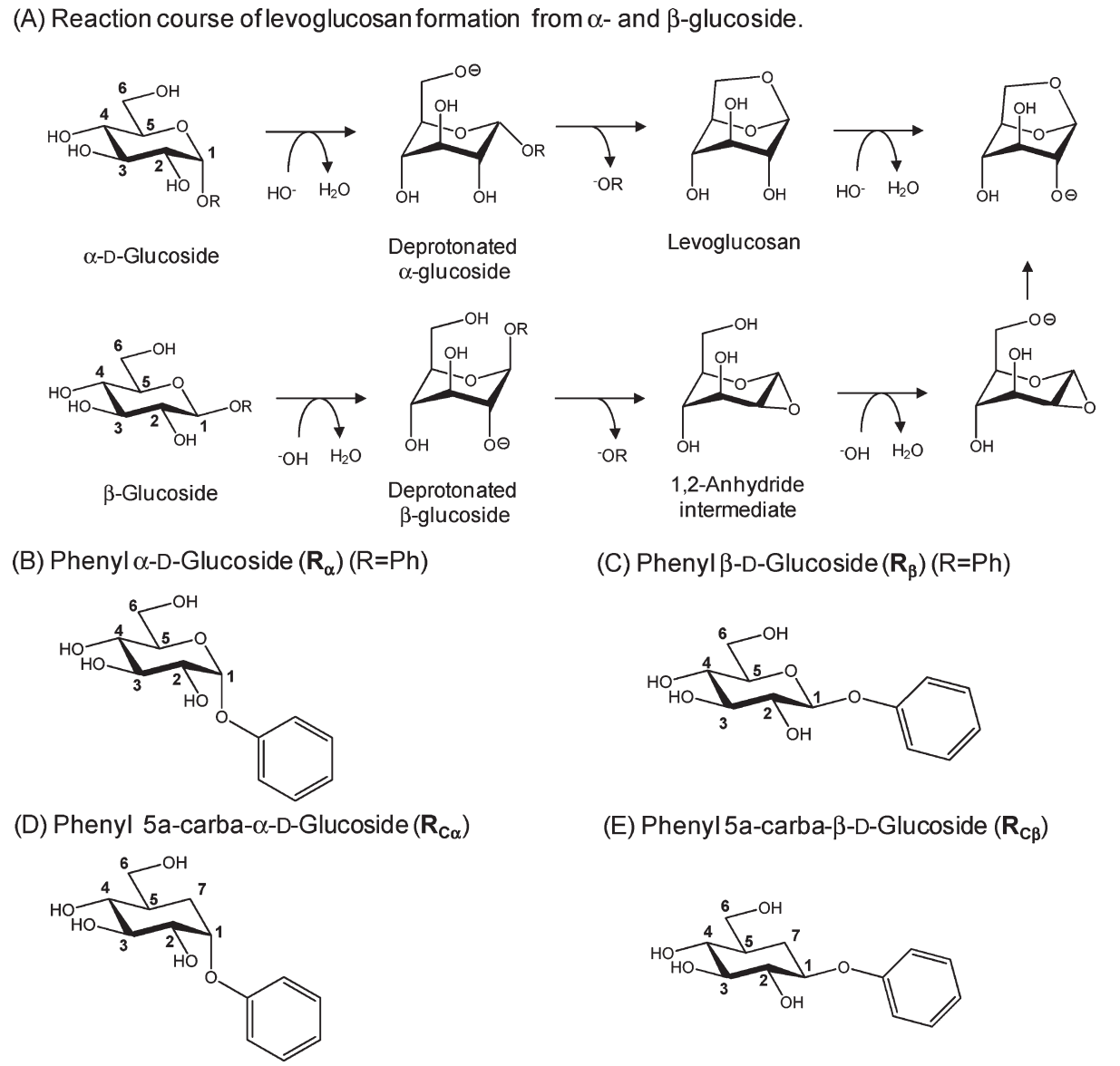

The initial step is proton transfer from the substrate OH group to bulk OH^- anion to form an oxyanion at the C2 atom. In the first intramolecular substitution, the C2-oxyanion attacks the C1 atom in a nucleophilic manner to induce the elimination of the OR^- group from the anomeric carbon, leading to the formation of 1,2-anhydride intermediate. This intermediate readily converts to levoglucosan through the second intramolecular substitution, in which the OH group at the C6 attacks the anomeric carbon in a nucleophilic manner. The formation of a similar 1,2-anhydride intermediate has been reported in many studies on alkaline degradations

(1) (a) Nevell, T. P. In *Cellulose Chemistry and its Applications*; Nevell, T. P., Zeronian, S. H., Eds.; Ellis Horwood, Chichester, UK, 1985; p 223. (b) Gentile, V. M.; Schroeder, L. R.; Atalla, R. H. In *the structures of cellulose - Characterisation of the solid states*, ACS Symp. Ser. No. 340; Atalla, R. H., Ed.; American Chemical Society, Washington, DC, 1987; p 272. (c) Ballou, C. E. *Adv. Carbohydr. Chem.* **1954**, *9*, 59–95. (d) Capon, B. *Chem. Rev.* **1969**, *69*, 429.
(2) Matthews, C. H. *Sven. Papperstidn.* **1974**, *77*, 629.
(3) Dimmel, D. R.; Willenbrink, H. J.; Vreede, P. V. *J. Wood Chem. Technol.* **2001**, *21*, 211.
(4) (a) Kaylor, R. M.; Dimmel, D. R.; Ragauskas, A. J.; Liotta, C. L. *J. Wood Chem. Technol.* **1995**, *15*, 431. (b) Schroeder, L. R.; Wylie, T. R. *J. Wood Chem. Technol.* **1998**, *18*, 107.
(5) Molinarolo, W. E.; Dimmel, D. R.; Malcolm, E. W.; Schroeder, L. R. *J. Wood Chem. Technol.* **1990**, *10*, 209.
(6) Moody, W.; Richards, G. N. *Carbohydr. Res.* **1981**, *93*, 83.
(7) Lai, Y. Z.; Ontto, D. E. *Carbohydr. Res.* **1979**, *75*, 51.
(8) (a) Blythe, D. A.; Schroeder, L. R. *J. Wood Chem. Technol.* **1985**, *5*, 313. (b) Lai, Y. Z. *Carbohydr. Res.* **1972**, *24*, 57. (c) Brooks, R. D.; Norman, S. T. *Tappi* **1966**, *49*, 362. (d) Best, E. V.; Green, J. W. *Tappi* **1969**, *52*, 1321.
(9) McCloskey, C. M.; Coleman, G. H. *J. Org. Chem.* **1945**, *10*, 184.
(10) Tsai, C. S.; Reyes-Zamora, C. *J. Org. Chem.* **1972**, *37*, 2725.
(11) (a) Gasman, R. C.; Johnson, D. C. *J. Org. Chem.* **1965**, *31*, 1830. (b) De Bruyue, C. K.; Wunendaele, F. V.; Carchon, H. *Carbohydr. Res.* **1974**, *33*, 75. (c) Lonnberg, H. *Acta Chem. Scand., Ser. A* **1977**, *31*, 265–270. (d) Kyosaka, S.; Murata, S.; Tanaka, M. *Chem. Pharm. Bull.* **1983**, *31*, 3902.
(12) Hall, A. N.; Hollingshead, S. *J. Chem. Soc.* **1961**, 4290.
(13) Lai, Y. Z.; Ontto, D. E. *Carbohydr. Res.* **1978**, *67*, 500.
(14) Ferriier, R. J.; Overend, W. G.; Ryan, A. E. *J. Chem. Soc.* **1965**, 3484.
(15) Robins, J. H.; Green, J. W. *Tappi* **1969**, *52*, 1346.
(16) (a) Tanaka, T.; Huang, W. C.; Noguchi, M.; Kobayashi, A.; Shoda, S. *Tetrahedron Lett.* **2009**, *50*, 2154. (b) Lu, S.; Li, X.; Wang, A. *Catal. Today* **2000**, *63*, 531.

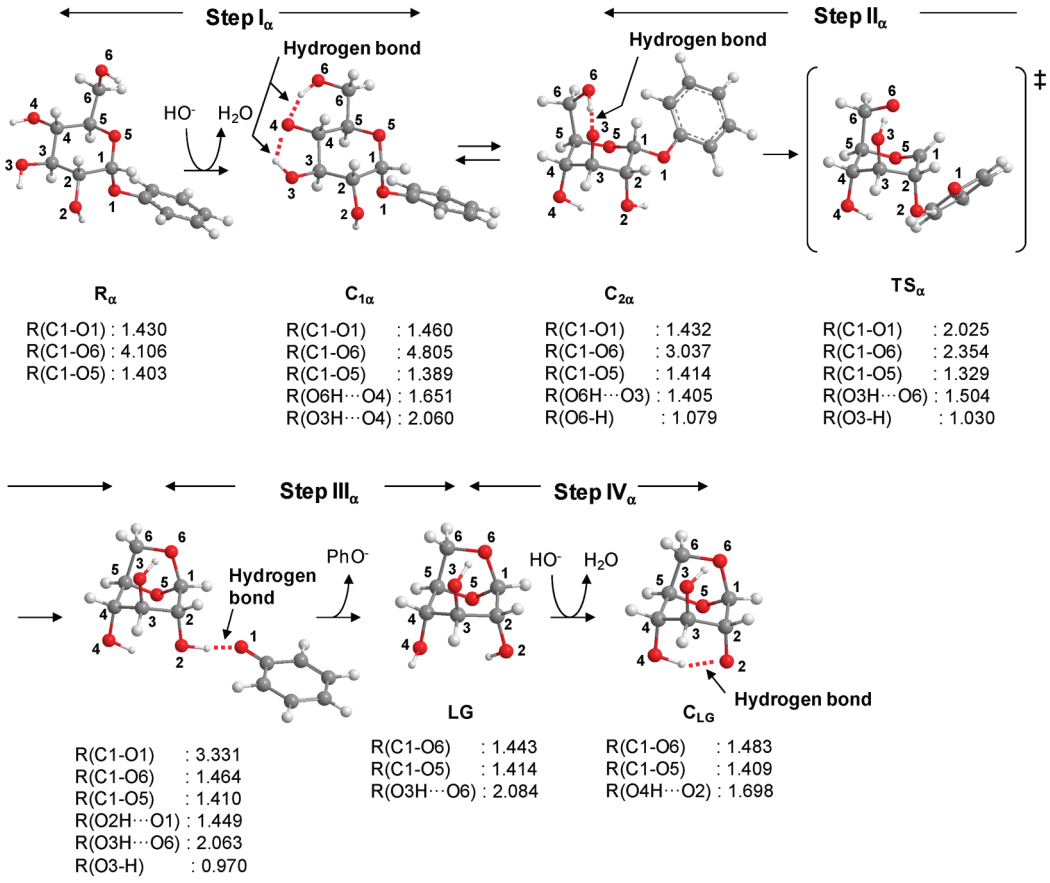

FIGURE 1. Geometry changes (DFT(B3LYP)/BS-I method) in the levoglucosan formation from phenyl α-D-glucoside ($\mathbf{R}_\alpha$).

of such glycosides as β-xyloside, β-galactoside, and α-mannoside whose OH group on the C2 takes the position trans to the aglycon.[9,11]

In the degradation of α-glucoside, on the other hand, the $S_N$icB(2) mechanism is not likely because the OH group on the C2 takes the position cis to the aglycon. Instead, the $S_N$icB mechanism was proposed, where the C6-oxyanion formed by the deprotonation of the OH group directly attacks the anomeric carbon to afford levoglucosan (see Scheme 1A).[7,9,12−15] This $S_N$icB mechanism is likely to work well, because the C6-oxyanion seems to easily approach the C1 in α-glucoside without a significantly large geometry change (see the deprotonated α-glucoside in Scheme 1A). Nevertheless, levoglucosan is produced from α-glucoside much more slowly with lower yields than that from the corresponding β-glucoside. The similar $S_N$icB mechanism was also proposed for degradation of many other glycosides whose OH group on the C2 atom is at the position cis to the aglycon like the α-glucoside.[9,11d] It is noted that all such glycosides exhibit low reactivity for 1,6-anhydrosugar formation

Though the reaction mechanisms of the levoglucosan formation from α- and β-glucosides have been investigated in many studies,[1−16] as described above, the reason for the difference in reactivity between α- and β-glucosides has not been elucidated yet, to our knowledge. The knowledge of the reason is indispensable to correctly understand the degradation of various glycosides under basic condition. The presence of the C2-oxyanion has been proposed as a plausible reason for the higher reactivity of β-glucosides, because the C2-oxyanion is a neighbor to the C1 (see Scheme 1A).[4−9] However, this proposal is not perfect to explain the lower reactivity of α-glucoside, because the C6-oxyanion in α-glucoside seems to more easily attack the C1 than the C2-oxyanion in β-glucoside does, as mentioned above.

In the present study, we theoretically investigated the levoglucosan formation from α- and β-glucosides with the MP4//DFT(B3LYP) method. Our purposes here are to understand well the reaction features and clarify the reasons why β-glucosides are more reactive than α-glucosides in the levoglucosan formation reaction.

2. Models and Computational Details

We employed phenyl α-D-glucoside ($\mathbf{R}_\alpha$) and phenyl β-D-glucoside ($\mathbf{R}_\beta$) as the models of real α- and β-D-glucosides, respectively (Scheme 1B,C), because these glucosides have been employed as substrates in many experimental works.[5−7,9,13] We also investigated phenyl 5a-carba-glucopyranosides ($\mathbf{R}_{C\alpha}$ and $\mathbf{R}_{C\beta}$; see Scheme 1D,E). The reasons for this investigation will be discussed below.

The MP4//DFT(B3LYP) method was used here since this method was successfully applied to similar reactions,

(17) (a) Motawia, M. S.; Olsen, C. E.; Moller, B. L.; Marcussen, J. *Carbohydr. Res.* **1994**, *252*, 69. (b) Gigg, R.; Penglis, A. A. E.; Conant, R. *J. Chem. Soc., Perkin Trans. 1* **1977**, 2014. (c) Perri, S. T.; Dyke, H. J.; Moore, H. W. *J. Org. Chem.* **1989**, *54*, 2034. (d) McDevitt, J. P.; Lansbury, P. T., Jr. *J. Am. Chem. Soc.* **1996**, *118*, 3818.
(18) Schuerch, C. *Adv. Carbohydr. Chem. Biochem.* **1981**, *39*, 157.
(19) Satoh, T.; Imai, T.; Ishihara, H.; Maeda, T.; Kitajyo, Y.; Sakai, Y.; Kaga, H.; Kaneko, N.; Ishii, F.; Kakuchi, T. *Macromolecules* **2005**, *38*, 4202.

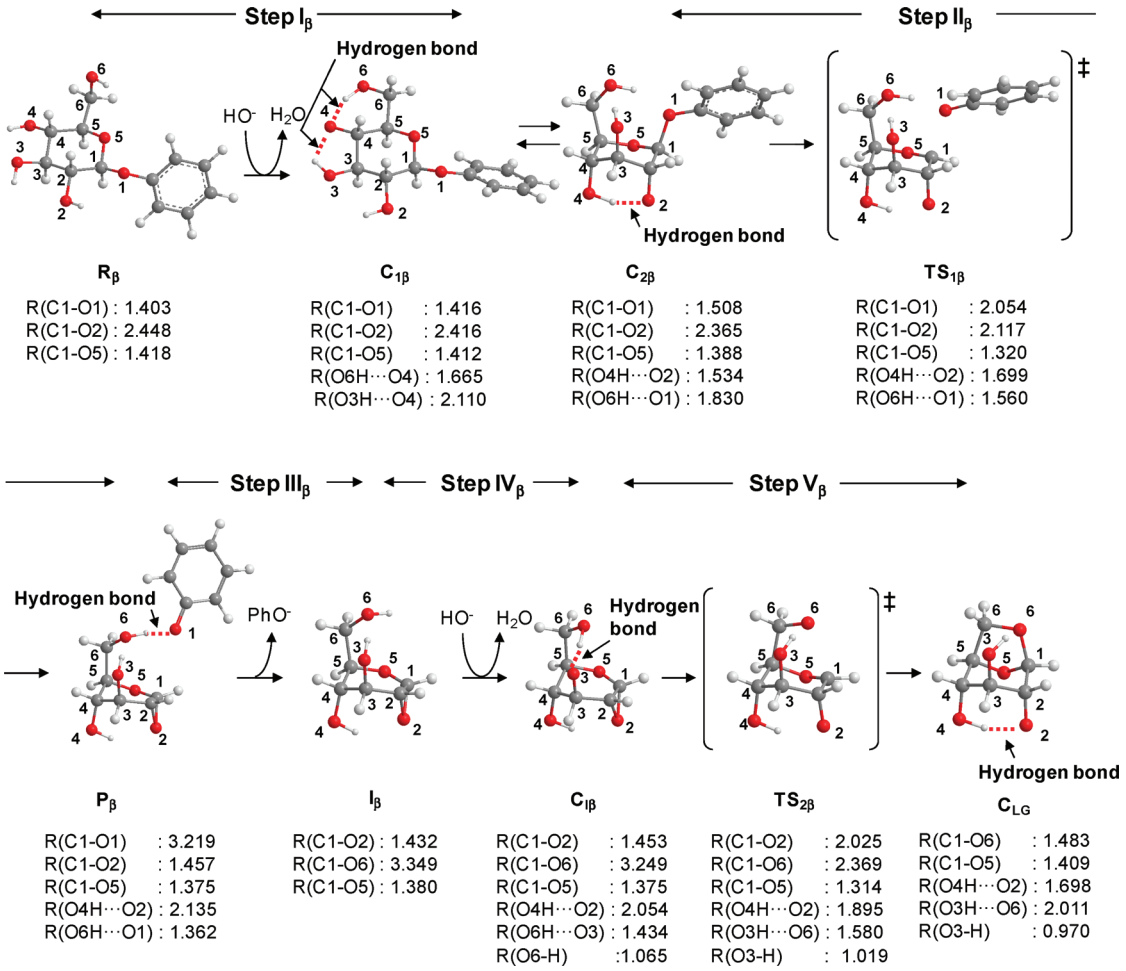

FIGURE 2. Geometry changes (DFT(B3LYP)/BS-I method) in the levoglucosan formation from phenyl β-D-glucoside ($\mathbf{R}_\beta$).

as reported in our recent study.[20] The geometry optimization was carried out by the DFT method with the B3LYP functional.[21] The 6-31G(d) basis sets were employed for H, C, and O, where a diffuse function was added to each of C and O and a p-polarization function was added to H of all OH groups. This basis set system is called BS-I, hereafter.

We reoptimized the geometries of the reactants, important intermediates, and transition states in water with the PCM method at the DFT(B3LYP)/BS-I level. This is called the DFT(B3LYP)-PCM method, hereafter. In the PCM calculation, the UFF parameters were used to determine the cavity size, where all hydrogen atoms are explicitly considered. The dielectric constant (ε) and the density (δ) of the solvent were taken to be the same as those of water at 373 K and 1 atm: $\varepsilon = 48$ and $\delta = 0.955$ g/cm^3. We ascertained that each equilibrium geometry exhibited no imaginary frequency and each transition state exhibited one imaginary frequency. Potential energy changes were evaluated by the MP4(SDQ) method with the DFT-optimized geometries, where a better basis set system (BS-II) was used. In BS-II, 6-311G(d) basis sets were used for all atoms, where a diffuse function was added to each of C and O and a p-polarization function was added to H of all OH groups, too.

Gibbs energy change (ΔG^0) was evaluated at 373 K, because the degradation experimentally occurs around this temperature.[6,7] In this evaluation, the potential energy change was calculated by the MP4(SDQ)/BS-II method and the solvation free energy was evaluated by the PCM method. Zero-point energy, thermal energy, and entropy changes were evaluated with the DFT(B3LYP)/BS-I method. The translational entropy in water was evaluated with the method in the literature.[22]

GAUSSIAN 03 and 09 program packages[23] were employed in these calculations. Pictures of molecular orbitals were drawn with the MOLEKEL program.[24]

3. Results and Discussion

3.1. Energy and Geometry Changes. Geometry changes in the reactions of levoglucosan formation from $\mathbf{R}_\alpha$ and $\mathbf{R}_\beta$ are preliminarily optimized with the DFT(B3LYP) method

(20) Hosoya, T.; Nakao, Y.; Sato, H.; Kawamoto, H.; Sakaki, S. *J. Org. Chem.* **2009**, *74*, 6891.

(21) (a) Becke, A. D. *Phys. Rev. A* **1988**, *38*, 3098. (b) Becke, A. D. *J. Chem. Phys.* **1983**, *98*, 5648.

(22) Mammen, M.; Shakhnovich, E. I.; Deutch, J. M.; Whitesides, G. M. *J. Org. Chem.* **1998**, *63*, 3821.

(23) (a) Pople, J. A. et al. *Gaussian 03*, Revision C.02; Gaussian, Inc., Wallingford, CT, 2004. See the Supporting Information for the complete reference. (b) Pople, J. A. et al. *Gaussian 09*, Revision A.02; Gaussian, Inc., Wallingford, CT, 2009. See the Supporting Information for the complete reference.

(24) Flükiger, P.; Lüthi, H. P.; Portann, S.; Weber, J. *MOLEKEL*, v.4.3; Scientific Computing, Manno, Switzerland, 2002−2002. Portman, S.; Lüthi, H. P. *Chimia* **2000**, *54*, 766.

TABLE 1. MP4(SDQ)-PCM//DFT(B3LYP)- and MP4(SDQ)-PCM//DFT(B3LYP)-PCM-Calculated Energies of Important Intermediates and Transition States

	ΔG^{0a} (kcal/mol)				
	R	**C_1**	**C_2**	**TS**	**P**
	(**A**) reaction of phenyl α-D-glucoside (**R_α**)				
MP4(SDQ)-PCM//DFT(B3LYP)	0.0 (0.0)	−9.9 (−10.6)	−8.8 (−10.6)	26.2 (24.9)	−17.5 (−16.8)
MP4(SDQ)-PCM//DFT(B3LYP)-PCM	0.0 (0.0)	−10.3 (−10.5)	−8.3 (−9.0)	27.9 (26.7)	−17.0 (−16.2)
	(**B**) reaction of phenyl β-D-glucoside (**R_β**)				
MP4(SDQ)-PCM//DFT(B3LYP)	0.0 (0.0)	−9.3 (−9.7)	−3.8 (−3.9)	14.6 (14.9)	−1.4 (0.5)
MP4(SDQ)-PCM//DFT(B3LYP)-PCM	0.0 (0.0)	−10.5 (−11.1)	−7.0 (−7.1)	15.1 (15.4)	−2.0 (0.2)

[a] ΔE values in parentheses.

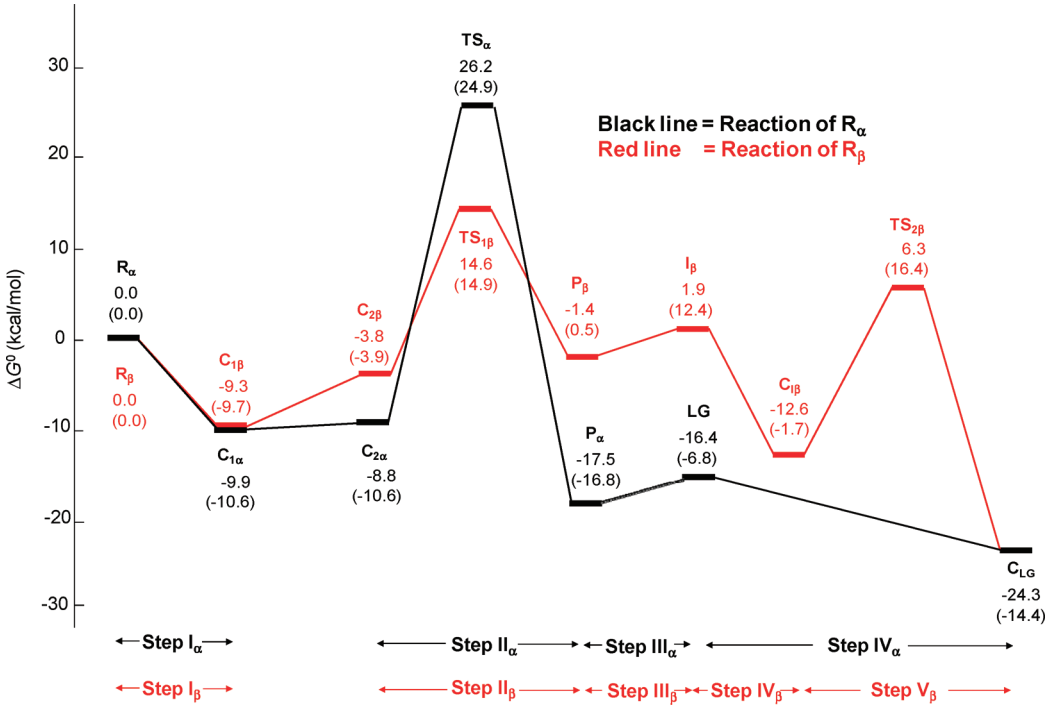

FIGURE 3. Gibbs energy changes (MP4(SDQ)-PCM/BS-II//DFT(B3LYP)/BS-I method) in the levoglucosan formation from phenyl α-D-glucoside (**R_α**) and phenyl β-D-glucoside (**R_β**). The ΔE value is given in parentheses.

without solvation effects, as shown in Figures 1 and 2. We reoptimized geometries of several important species with the DFT(B3LYP)-PCM method and found that solvation with water induces little geometry change (see Figures S1 and S2 in the Supporting Information). Also, the energy changes evaluated with the MP4(SDQ)-PCM method are little different between the geometries optimized with DFT(B3LYP) and DFT(B3LYP)-PCM methods, as shown in Table 1. These results indicate that reliable discussion can be presented based on the MP4(SDQ)-PCM-evaluated energy changes with the geometries optimized in the gas phase.

The initial step of the levoglucosan formation from **R_α** and **R_β** is deprotonation of the OH group to afford oxyanions **C_α** and **C_β**. This deprotonation is named steps I_α and I_β for the reactions of **R_α** and **R_β**, respectively (see Figures 1 and 2). The nucleophilic substitution was reported to start from the C6-oxyanion bearing the $^1C_4$ conformation in the reaction of **R_α** and from the C2-oxyanion bearing the $^1C_4$ conformation in the reaction of **R_β**.[25] We first investigated these two oxyanions. The geometry optimization of the C6-oxyanion of **R_α** bearing the $^1C_4$ conformation leads to the C3-oxyanion **$C_{2\alpha}$** through the proton transfer from the O3 to the O6 (see Figure 1 for **$C_{2\alpha}$** and Figure S3 in the Supporting Information for the geometries before and after the geometry optimization). This result indicates that the C6-oxyanion ($^1C_4$) of **R_α** does not exist even in a local minimum and that the C3-oxyanion ($^1C_4$) is more stable than the C6-oxyanion ($^1C_4$).[26] In the deprotonated **R_β**, the C2-oxyanion **$C_{2\beta}$** bearing the $^1C_4$ conformation was optimized, indicating that the C2-oxyanion is a stable species (see Figure 2 for **$C_{2\beta}$** and Figure S3 in the Supporting Information for the geometries before and after the geometry optimization). To find the most stable oxyanion, we also

(25) The intramolecular substitution was discussed to occur from the $^1C_4$ conformer, because the nucleophilic center takes the position behind the C1−O1 bond of the $^1C_4$ conformer in both α- and β-anomers; see refs 1d, 4b, and 5.

(26) Because we investigated the C6-oxyanion only in $^1C_4$ and $^4C_1$ conformations, the present result does not rule out the possibility that the C6-oxyanion exists to a minor extent in the equilibrium with other conformations.

investigated all possible C2-, C3-, C4-, and C6-oxyanions bearing the $^4C_1$ conformation, because the $^4C_1$ conformer is generally more stable than the $^1C_4$ conformer. ΔG^0 values for all optimized oxyanions were calculated with the MP4(SDQ)-PCM method to be considerably negative, indicating that the deprotonation of the OH group easily occurs to form these oxyanions (see Figures 3 and S3, Supporting Information).[27] The C4-oxyanions ($^4C_1$), $\mathbf{C_{1\alpha}}$ and $\mathbf{C_{1\beta}}$, were found to be the most stable and the stability decreases in the following order: C4-oxyanion ($^4C_1$) > C3-oxyanion ($^1C_4$) > C2-oxyanion ($^4C_1$) in the oxyanions of $\mathbf{R_\alpha}$ and C4-oxyanion ($^4C_1$) > C2-oxyanion ($^4C_1$) > C2-oxyanion ($^1C_4$) in the oxyanions of $\mathbf{R_\beta}$ (see Figure S3 in the Supporting Information). This is because the O6H and O3H groups form hydrogen bonds with the anionic O4 in these C4-oxyanions ($^4C_1$), $\mathbf{C_{1\alpha}}$ and $\mathbf{C_{1\beta}}$ (see Figures 1 and 2).

It is likely that $\mathbf{C_{1\alpha}}$ and $\mathbf{C_{1\beta}}$ bearing the $^4C_1$ conformation are in equilibrium with $\mathbf{C_{2\alpha}}$ and $\mathbf{C_{2\beta}}$ bearing the $^1C_4$ conformation in water solution; actually, the conformational change from $\mathbf{C_{1\alpha}}$ to $\mathbf{C_{2\alpha}}$ and that from $\mathbf{C_{1\beta}}$ to $\mathbf{C_{2\beta}}$ occur with moderate $\Delta G^{0\ddagger}$ values of 15.3 and 18.0 kcal/mol, respectively, where the MP4(SDQ)-PCM/BS-II//DFT(B3LYP)/BS-I method was employed (see Figure S4 in the Supporting Information for geometry and energy changes). Several theoretical studies also reported that similar conformational changes of the pyranosyl ring easily occur.[20,28] On the basis of these results, we will investigate the reaction of $\mathbf{R_\alpha}$ starting from $\mathbf{C_{2\alpha}}$ and that of $\mathbf{R_\beta}$ starting from $\mathbf{C_{2\beta}}$.

In the degradation of $\mathbf{R_\alpha}$, the intramolecular nucleophilic attack of the C6-oxyanion to the C1 atom occurs starting from $\mathbf{C_{2\alpha}}$ to afford a product complex $\mathbf{P_\alpha}$ through transition state $\mathbf{TS_\alpha}$, as shown by step II_α in Figure 1. The geometry search starting from $\mathbf{TS_\alpha}$ clearly indicated that $\mathbf{TS_\alpha}$ connects $\mathbf{C_{2\alpha}}$ and $\mathbf{P_\alpha}$.[29] In this step, as the O6 atom approaches the C1 atom, the H atom transfers from the O6 atom to the O3 atom as proton to afford the C6-oxyanion. In $\mathbf{TS_\alpha}$, this proton transfer has been almost completed. In $\mathbf{P_\alpha}$, the phenoxy anion is bound with levoglucosan through the hydrogen bond. The $\Delta G^{0\ddagger}$ and E_a values are 36.1 and 35.5 kcal/mol, respectively, relative to the most stable $\mathbf{C_{1\alpha}}$ (see Figure 3). This process is the rate-determining step in the overall reaction, as clearly seen in Figure 3, which provides theoretical support to the experimental proposal.[7,13] It is noted that the E_a value of this process converges when going to MP4(SDQ) from MP2, indicating that the MP4(SDQ) method exhibits a reliable E_a value (see Table S1 in the Supporting Information). $\mathbf{P_\alpha}$ subsequently releases phenoxy anion to yield levoglucosan (**LG**) (see step III_α in Figure 1). This process is endothermic ($\Delta G^0 = 1.1$ kcal/mol, $\Delta E = 10.0$ kcal/mol); note that the increase in the ΔG^0 value is much smaller than that in the ΔE value because of the increase in entropy (see Figure 3). Levoglucosan finally undergoes deprotonation to produce the C2-oxyanion $\mathbf{C_{LG}}$ (step IV_α in Figure 1), where $\mathbf{C_{LG}}$ (C2-oxyanion) is the most stable in all oxyanions of **LG**.[30] The total reaction energy of the $\mathbf{C_{LG}}$ formation from $\mathbf{C_{2\alpha}}$ is exothermic: $\Delta G^0 = -14.4$ kcal/mol and $\Delta E = -3.8$ kcal/mol, as shown in Figure 3.

TABLE 2. MP4(SDQ)-PCM//DFT(B3LYP)-calculated and experimental $\Delta H^{0\ddagger}$ values of the Steps II_α and II_β[a]

	$\Delta H^{0\ddagger}$ (kcal/mol)	
	calcd	exptl
phenyl α-D-glucoside ($\mathbf{R_\alpha}$)	34.8 (36.6)[b]	17.9[c]
phenyl β-D-glucoside ($\mathbf{R_\beta}$)	24.2 (25.7)	23.2,[c] 28.3[d]

[a]See Figures 1 and 2. [b]The $\Delta H^{0\ddagger}$ value calculated with the geometries optimized by the DFT(B3LYP)-PCM method (water) is in parentheses. [c]Reference 7. [d]Reference 5.

In the degradation of $\mathbf{R_\beta}$, the intramolecular nucleophilic attack of the C2-oxyanion to the C1 atom occurs starting from $\mathbf{C_{2\beta}}$ to form a product complex $\mathbf{P_\beta}$ via transition state $\mathbf{TS_{1\beta}}$, as shown by step II_β in Figure 2. In $\mathbf{P_\beta}$, the phenoxy anion is bound with the 1,2-anhydride intermediate. The $\Delta G^{0\ddagger}$ and E_a values of this process are 23.9 and 24.6 kcal/mol, respectively, relative to the most stable $\mathbf{C_{1\beta}}$, as shown in Figure 3. These $\Delta G^{0\ddagger}$ and E_a values are much lower than those of the levoglucosan formation starting from $\mathbf{R_\alpha}$, as shown by Figure 3: $\Delta G^{0\ddagger} = 36.1$ kcal/mol and $E_a = 35.5$ kcal/mol. This result is consistent with the experimental observation that the degradation of $\mathbf{R_\beta}$ much more rapidly occurs than that of $\mathbf{R_\alpha}$.[1,7,9] $\mathbf{P_\beta}$ releases phenoxy anion to produce the 1,2-anhydride intermediate $\mathbf{I_\beta}$ (see step III_β in Figure 2). In $\mathbf{I_\beta}$, the deprotonation of the O3H group occurs to form C3-oxyanion $\mathbf{C_{1\beta}}$ (see step IV_β in Figure 2).[31] $\mathbf{C_{1\beta}}$ further undergoes the second intramolecular substitution to produce $\mathbf{C_{LG}}$ via transition state $\mathbf{TS_{2\beta}}$ (see step V_β in Figure 2). This step occurs concomitantly with the proton transfer from the O6 to the O3, similar to that in step II_α (see Figures 1 and 2 for detailed geometry changes). The $\Delta G^{0\ddagger}$ and E_a values (18.9 and 18.1 kcal/mol, respectively) of this step are much smaller than those of the first nucleophilic attack (23.9 and 24.6 kcal/mol), respectively, as shown by Figure 3, indicating that the first intramolecular substitution is the rate-determining step. These results are consistent with previous experimental results.[4−9] The exothermicity of the reaction of $\mathbf{R_\beta}$ ($\Delta G^0 = -15.0$ kcal/mol and $\Delta E = -4.7$ kcal/mol) is similar to that ($\Delta G^0 = -14.4$ kcal/mol and $\Delta E = -3.8$ kcal/mol) of the reaction of $\mathbf{R_\alpha}$ (see Figure 3).

The calculated $\Delta H^{0\ddagger}$ value of the reaction of $\mathbf{R_\beta}$ agrees well with the experimental value, as compared in Table 2.[32] On the other hand, the calculated $\Delta H^{0\ddagger}$ value of the reaction of $\mathbf{R_\alpha}$ is considerably different from the experimental one. This is probably because the alkaline degradation of $\mathbf{R_\alpha}$ occurs with some side reactions besides the levoglucosan formation and hence the experimental $\Delta H^{0\ddagger}$ value contains the $\Delta H^{0\ddagger}$ values for the side reactions. This is supported by the fact

(27) We compare the sum of the energies of **R** and OH^- to that of $\mathbf{C_1}$ and H_2O. Though the isolated OH^- molecule is not realistic in water solution, the solvation of OH^- in water is considered to be similar to that of $\mathbf{C_1}$.

(28) (a) Biarnés, X.; Ardévol, A.; Planas, A.; Rovira, C.; Laio, A.; Parrinello, M. *J. Am. Chem. Soc.* **2007**, *129*, 10686. (b) Ionescu, A. R.; Bérces, A.; Zgierski, M. Z.; Whitfield, D. M.; Nukada, T. *J. Phys. Chem. A* **2005**, *109*, 8096. (c) O'Donoghue, P.; Luthey-Schulten, Z. A. *J. Phys. Chem. B* **2000**, *104*, 10398. (d) Kurihara, Y.; Ueda, K. *Carbohydr. Res.* **2006**, *341*, 2565.

(29) We employed here the geometry optimization with the steepest descend technique that approximately corresponds to the IRC calculation, because the IRC calculation is time consuming. The geometry optimization starting from $\mathbf{TS_\alpha}$ reaches $\mathbf{C_{2\alpha}}$ and $\mathbf{P_\alpha}$, indicating that $\mathbf{TS_\alpha}$ connects $\mathbf{C_\alpha}$ ($^1C_4$) and $\mathbf{P_\alpha}$.

(30) The ΔG^0 of the C3-oxyanion is 2.4 kcal/mol larger than that of $\mathbf{C_{LG}}$. The optimization of the C4-oxyanin leads to $\mathbf{C_{LG}}$, indicating that the C4-oxyanion is not an equilibrium species.

(31) The ΔG^0 of the C4-oxyanion of $\mathbf{I_\beta}$ is 14.2 kcal/mol higher than that of $\mathbf{C_{1\beta}}$.

(32) Experimental $\Delta G^{0\ddagger}$ values are also reported in refs 5 and 7. However, we employ $\Delta H^{0\ddagger}$ values here, because the $\Delta S^{0\ddagger}$ value is only approximately estimated in solution.

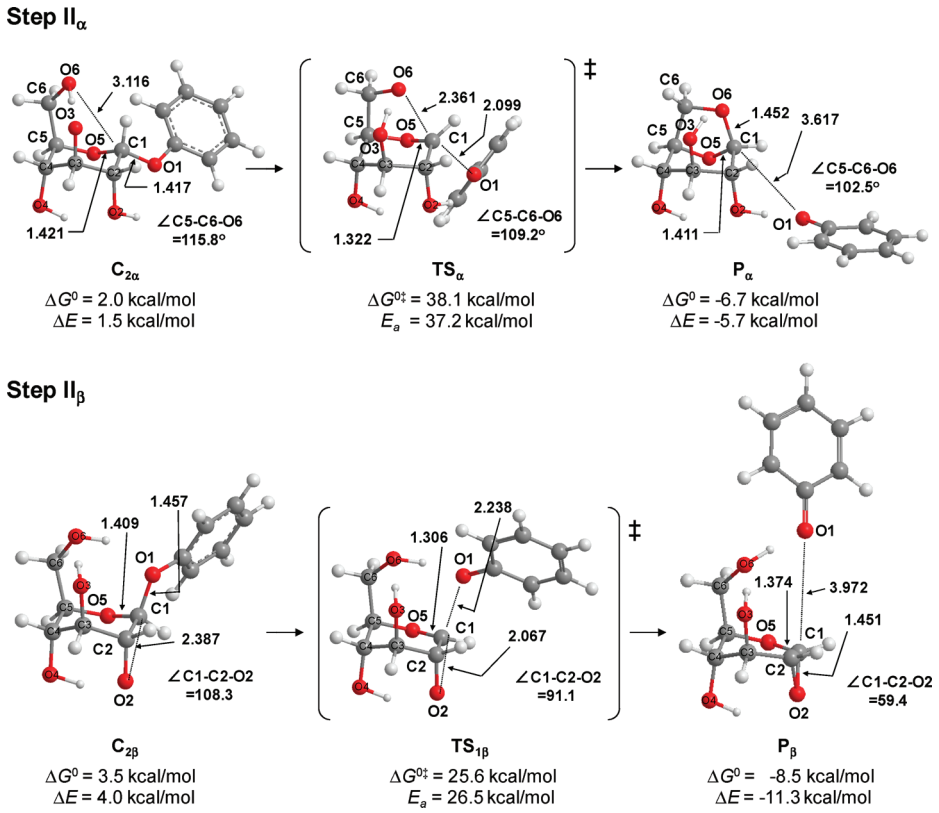

FIGURE 4. Changes of the geometry and the Gibbs energy (relative to the most stable C4-oxyanions $\mathbf{C_{1\alpha}}$ and $\mathbf{C_{1\beta}}$) in steps II_α and II_β. The MP4(SDQ)-PCM/BS-II//DFT(B3LYP)-PCM/BS-I method was employed.

that the yield of levoglucosan from $\mathbf{R_\alpha}$ was much lower than the conversion.[13] Thus, the computed $\Delta H^{0‡}$ value cannot be compared with the experimental value.

3.2. Origin of the Difference in Reactivity between α- and *β*-Glucosides. Here, we wish to discuss details of the first intramolecular nucleophilic attack of the oxyanion to the C1 (steps II_α and II_β in Figures 1, 2, and 3) because this is the rate-determining step. We employed reoptimized geometries with the DFT(B3LYP)-PCM method; though the solvation effect by water is not large, as mentioned above, there is no reason to use geometries optimized in water.

In step II_α of the $\mathbf{R_\alpha}$ reaction, the C1−O1 bond lengthens to 2.099 Å from 1.417 Å and the C1−O6 distance simultaneously shortens to 2.361 Å from 3.116 Å when going to $\mathbf{TS_\alpha}$ from $\mathbf{C_{2\alpha}}$, as shown in Figure 4. After $\mathbf{TS_\alpha}$, the C1−O1 bond further lengthens to 3.617 Å and simultaneously the C1−O6 distance further shortens to 1.452 Å to form the C1−O6 covalent bond in $\mathbf{P_\alpha}$. The C5−C6−O6 angle moderately decreases from 115.8° to 109.2° when going to $\mathbf{TS_\alpha}$ from $\mathbf{C_{2\alpha}}$ and finally it becomes 102.5° in $\mathbf{P_\alpha}$. These geometry changes indicate that this reaction occurs via the S_N2-type mechanism. In step II_β of the $\mathbf{R_\beta}$ reaction, on the other hand, the C1−O2 distance somewhat shortens to 2.067 Å from 2.387 Å when going to $\mathbf{TS_{1\beta}}$ from $\mathbf{C_{2\beta}}$, while the C1−O1 bond considerably lengthens to 2.238 Å from 1.457 Å. The C1−C2−O2 angle also moderately decreases from 108.3° to 91.1° when going to $\mathbf{TS_{1\beta}}$, against our expectation that this angle considerably decreases with the formation of the three-membered ring. After $\mathbf{TS_{1\beta}}$, the C1−O2 distance considerably shortens to 1.451 Å concomitantly with the considerably large decrease in the C1−C2−O2 angle to 59.4°. These results

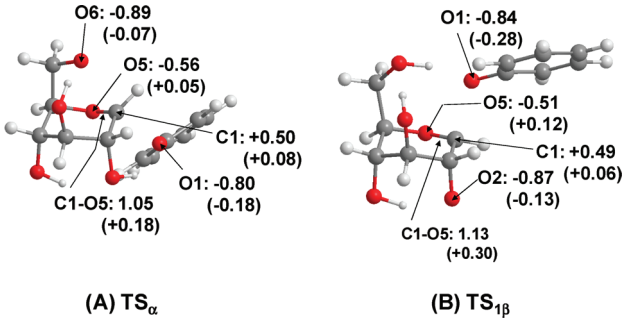

FIGURE 5. NBO charges and bond orders (MP4(SDQ)/BS-II//DFT(B3LYP)-PCM/BS-I method) of $\mathbf{TS_\alpha}$ and $\mathbf{TS_{1\beta}}$. The differences from $\mathbf{C_{1\alpha}}$ in $\mathbf{TS_\alpha}$ and those from $\mathbf{C_{1\beta}}$ in $\mathbf{TS_{1\beta}}$ are in parentheses.

indicate that the C1−O1 bond breaking mainly occurs before $\mathbf{TS_{1\beta}}$ and the C1−O2 bond formation mainly occurs after $\mathbf{TS_{1\beta}}$. Thus, step II_β is understood to be the S_N1-type reaction rather than the S_N2-type one. This understanding is supported by recent experimental studies showing that 2-thioalkyl/aryl sugars form oxacarbenium ions in their acid-catalyzed glycosidic bond cleavage but not sulfonium ion species.[33] We found the other S_N1-type reaction course, where the attack of the O6 to the C1 directly forms levoglucosan. However, this reaction requires a much higher activation barrier than step II_β, indicating that this direct levoglucosan formation is unfavorable (see Figure S5 in the Supporting Information).

(33) (a) Hou, D.; Taha, H. A.; Lowary, T. L. *J. Am. Chem. Soc.* **2009**, *131*, 12937. (b) Beaver, M.; Billings, S.; Woerpel, K. *Eur. J. Org. Chem.* **2008**, 771.

The S_N1 reaction generally needs considerable stabilization of the cationic center by charge transfer (CT) from the adjacent group. Such CT reflects in the NBO charge and the bond order of $\mathbf{TS_{1\beta}}$ and $\mathbf{TS_{\alpha}}$. As shown in Figure 5, the atomic charge of the O5 is less negative in $\mathbf{TS_{1\beta}}$ (−0.51) than in $\mathbf{TS_{\alpha}}$ (−0.56). The C1−O5 bond order (1.13) of $\mathbf{TS_{1\beta}}$ is also larger than that (1.05) of $\mathbf{TS_{\alpha}}$. When going from $\mathbf{C_{1\alpha}}$ and $\mathbf{C_{1\beta}}$ to $\mathbf{TS_{\alpha}}$ and $\mathbf{TS_{1\beta}}$, respectively, the O5 charge becomes less negative by 0.12 e in the reaction of $\mathbf{R_{\beta}}$ than in that of $\mathbf{R_{\alpha}}$ by 0.05 e and the C1−O5 bond order more increases by 0.30 in the reaction of $\mathbf{R_{\beta}}$ than in that of $\mathbf{R_{\alpha}}$ by 0.18. All these results indicate that the CT from the O5 to the C1 more strongly occurs in $\mathbf{TS_{1\beta}}$ than in $\mathbf{TS_{\alpha}}$.[34] It is also noted that the shorter C1−O5 distance in $\mathbf{TS_{1\beta}}$ than in $\mathbf{TS_{\alpha}}$ indicates the stronger CT interaction in $\mathbf{TS_{1\beta}}$ (see Figure 4).

To understand well the CT from the O5 to the C1 in the transition states, we investigated important molecular orbitals of $\mathbf{TS_{\alpha}}$ and $\mathbf{TS_{1\beta}}$. Here, the OPh group was omitted to inspect the glucosyl moiety and simple models $\mathbf{TS_{\alpha}}'$ and $\mathbf{TS_{1\beta}}'$ were investigated, because the OPh group little influences the difference in the CT from the O5 to the C1 between $\mathbf{TS_{\alpha}}$ and $\mathbf{TS_{1\beta}}$ (see Figure S6 in the Supporting Information). As shown in Figure 6, the HOMO-15[35] of $\mathbf{TS_{1\beta}}'$ mainly consists of the lone pair of the O5, which overlaps with the p-orbital of the C1 in a bonding way. The antibonding counterpart of this bonding orbital appears in the LUMO. The HOMO-18 and the LUMO of $\mathbf{TS_{\alpha}}'$ correspond to the HOMO-15 and the LUMO of $\mathbf{TS_{1\beta}}'$, respectively. In the HOMO-18,[35] the empty p-orbital of the C1 mixes in a bonding way much less with the lone pair of the O5 than in the HOMO-15 of $\mathbf{TS_{1\beta}}'$. This is because the lone pair of the O5 is not parallel to the empty p-orbital of the C1 in $\mathbf{TS_{\alpha}}$ but almost parallel in $\mathbf{TS_{1\beta}}$, as shown in Scheme 2. The similar stereoelectronic effect has been proposed to explain the difference in reactivity between α- and β-anomers in acid- and enzyme-catalyzed hydrolyses and syntheses of glycosides,[36] though direct evidence was not presented. It is noted that our results provide theoretical evidence of the stereoelectronic effect and its reasons.

3.3. Intramolecular Nucleophilic Substitution Reactions of Phenyl 5a-Carba-glucopyranosides. Here, we investigated the intramolecular nucleophilic substitution step (I-C_{α} and I-C_{β}) of phenyl 5a-carba-glucopyranosides, $\mathbf{R_{C\alpha}}$ and $\mathbf{R_{C\beta}}$, which contain a methylene group instead of the O5 (see Scheme 1D, E). We investigated these compounds because the methylene group induces little stereoelectronic effect due to the absence of the lone pair orbital. Because the geometries of $\mathbf{R_{C\alpha}}$, $\mathbf{R_{C\beta}}$, and their deprotonated species ($\mathbf{C_{C\alpha}}$ and $\mathbf{C_{C\beta}}$) are similar to those of phenyl glucosides, the comparison between phenyl glucosides and phenyl 5a-carba-glucopyranosides is expected to indicate how important the stereoelectronic effect of the O5 is (see geometries of $\mathbf{C_{2C\alpha}}$ and $\mathbf{C_{2C\beta}}$ in Figure 7 and those

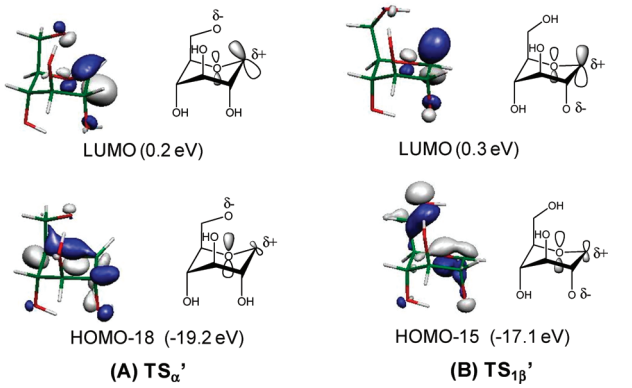

FIGURE 6. Important molecular orbitals of $\mathbf{TS_{\alpha}}'$ and $\mathbf{TS_{1\beta}}'$, where the OPh group is removed from $\mathbf{TS_{\alpha}}$ and $\mathbf{TS_{1\beta}}$ for brevity. The geometries of these species were taken to be the same as the corresponding geometries of $\mathbf{TS_{\alpha}}$ and $\mathbf{TS_{1\beta}}$. Note that the pyranosyl ring conformations of $\mathbf{TS_{\alpha}}'$ and $\mathbf{TS_{1\beta}}'$ are almost the same as those of the canonical $^1C_4$ one. For the values in parentheses the HF/BS-II//DFT(B3LYP)-PCM/BS-I method was employed. See ref 35 for HOMO-18 and HOMO-15.

SCHEME 2. Schematic Pictures of Orbital Interaction between the Lone Pair Orbital of the O5 and the Empty p-Orbital of the C1

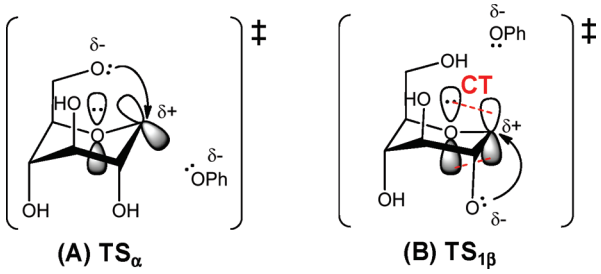

of $\mathbf{C_{1C\alpha}}$ and $\mathbf{C_{1C\beta}}$, $\mathbf{R_{C\alpha}}$, and $\mathbf{R_{C\alpha}}$ in Figure S7 in the Supporting Information).

In step I-C_{α}, $\mathbf{C_{2C\alpha}}$ changes to $\mathbf{P_{C\alpha}}$ via $\mathbf{TS_{C\alpha}}$, as shown in Figure 7, and in step I-C_{β}, $\mathbf{C_{2C\beta}}$ changes to $\mathbf{P_{C\beta}}$ via $\mathbf{TS_{C\beta}}$. Because these steps correspond to steps II_{α} and II_{β} in Figure 4, respectively, the geometry and energy changes will be compared with those of steps II_{α} and II_{β}. Actually, $\mathbf{TS_{C\alpha}}$ is similar to $\mathbf{TS_{\alpha}}$ (see also the Supporting Information, p S11). Consistent with these geometrical features, the activation barrier for $\mathbf{TS_{C\alpha}}$ is little different from that for $\mathbf{TS_{\alpha}}$ (see Figures 4 and 7). These similar characters of $\mathbf{TS_{\alpha}}$ and $\mathbf{TS_{C\alpha}}$ clearly indicate that the CT interaction between the O5 and C1 is little formed in $\mathbf{TS_{\alpha}}$, and hence, $\mathbf{TS_{\alpha}}$ is little stabilized by the CT interaction, leading to the similar $\Delta G^{0\ddagger}$ values of these two reactions. In $\mathbf{TS_{C\beta}}$, on the other hand, the C1−O1 distance is considerably shorter and the C1−O2 distance is moderately shorter than those of $\mathbf{TS_{1\beta}}$. The C1−C2−O2 angle of $\mathbf{TS_{C\beta}}$ is also considerably smaller than that of $\mathbf{TS_{1\beta}}$. These geometrical features indicate that $\mathbf{TS_{C\beta}}$ is understood to be the transition state of the S_N2-type reaction. Consistent with this S_N2-type transition state, the activation barrier for $\mathbf{TS_{C\beta}}$ becomes considerably larger than that for $\mathbf{TS_{1\beta}}$, as shown in Figures 4 and 7. All these results arise from the fact that the S_N1-type transition state is not stable here because of the absence of the O5 lone pair orbital; if the O5 lone pair orbital was present, it stabilized the S_N1-type transition state

(34) Contrary to the O5 charge, the C1 charge is similar between $\mathbf{TS_{\alpha}}$ and $\mathbf{TS_{1\beta}}$. This is because not only the CT from the O5 but those from the nucleophilic oxygen and the leaving group also affect the charge of the C1.

(35) The HOMO-*n* represents the *n*th MO counting from the HOMO toward the low-energy direction.

(36) (a) Tvaroška, I.; Bleha, T. *Adv. Carbohydr. Chem. Biochem.* **1989**, *47*, 45. (b) *The Anomeric Effect and Associated Stereoelectronic Effects*; ACS Symp. Ser. No. 539; Thatcher, G. R. J., Ed.; American Chemical Society: Washington, DC, 1993. (c) Sinnott, M. L. *Adv. Phys. Org. Chem.* **1988**, *24*, 113–204. (d) Sinnott, M. L. *Chem. Rev.* **1990**, *90*, 1171. (e) Mydock, L. K.; Demchenko, A. V. *Org. Biomol. Chem.* **2010**, *8*, 497.

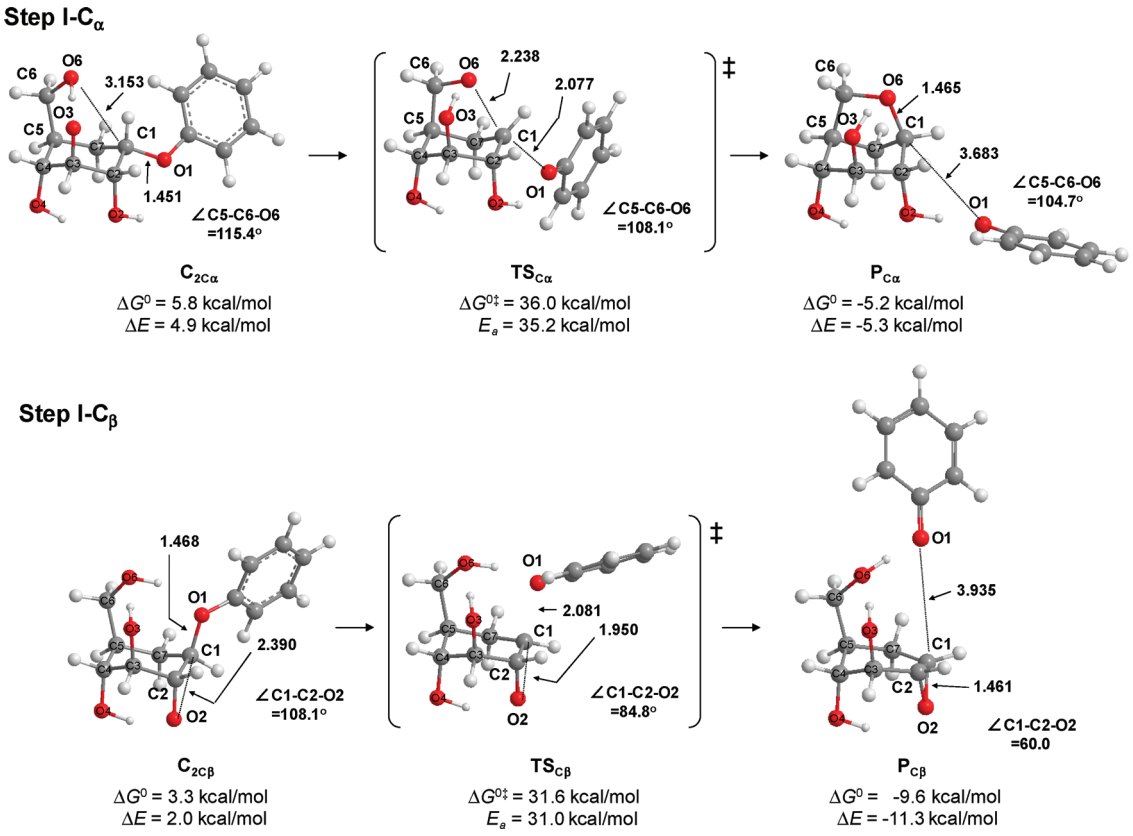

FIGURE 7. Changes of the geometry and the Gibbs energy (presented relative to the most stable C4-oxyanions bearing the $^4C_1$ conformation, $\mathbf{C_{1C\alpha}}$ and $\mathbf{C_{1C\beta}}$) in the reactions of phenyl 5a-carba-glucosides. The MP4(SDQ)-PCM/BS-II//DFT(B3LYP)- PCM/BS-I method was employed.

by the CT interaction. Thus, it is concluded that the stereoelectronic effect by the O5 lone pair is responsible for the higher reactivity of the β-anomer.

On the basis of the difference in the activation barrier between $\mathbf{TS_{C\beta}}$ and $\mathbf{TS_{1\beta}}$, the stereoelectronic effect of the O5 is estimated to be about 6.0 kcal/mol in Gibbs energy and 4.5 kcal/mol in potential energy. These values are about 50% of the difference in $\Delta G^{0\ddagger}$ and E_a values between $\mathbf{TS_\alpha}$ and $\mathbf{TS_{1\beta}}$. However, the stereoelectronic effect is underestimated here, because the C1···O1 electrostatic interaction is stronger in $\mathbf{TS_{C\beta}}$ than in $\mathbf{TS_{1\beta}}$ to compensate the absence of the stereoelectronic effect in $\mathbf{TS_{C\beta}}$ (see Figures 4 and 7 for the shorter C1−O1 distance in $\mathbf{TS_{C\beta}}$ than in $\mathbf{TS_{1\beta}}$). When the C1−O1 distance of $\mathbf{TS_{C\beta}}$ is elongated to 2.238 Å as in $\mathbf{TS_{1\beta}}$, the energy difference moderately increases to 7.0 kcal/mol in Gibbs energy and 5.6 kcal/mol in potential energy. These values are about 60% of the difference in $\Delta G^{0\ddagger}$ and E_a values between α- and β-glucosides, indicating that the stereoelectronic effect is one of the major origins of the higher reactivity of β-anomer for alkaline degradation.

The above results suggest that other factors are responsible for the higher reactivity of $\mathbf{R_\beta}$ than that of $\mathbf{R_\alpha}$. The H−C1−C2−H dihedral angle is one of these factors. This dihedral angle is 51.2° in $\mathbf{TS_{1\beta}}$ but 3.0° in $\mathbf{TS_\alpha}$, indicating that the C1−H and C2−H bonds are almost eclipsed in $\mathbf{TS_\alpha}$ but staggered in $\mathbf{TS_{1\beta}}$. A similar difference in the H−C1−C2−H dihedral angle is observed between $\mathbf{TS_{1\beta}}$ (51.2°) and that of $\mathbf{TS_\alpha}$ (4.8°). The eclipsed conformation around the C1−C2 bond of $\mathbf{TS_\alpha}$ is also one of the origins of the low reactivity of α-glucoside.

4. Conclusions

Present MP4(SDQ)//DFT(B3LYP) computations clearly show that the degradation of α-glucoside occurs through the $S_N$icB mechanism but that of β-glucoside occurs through the $S_N$icB(2) mechanism. The reaction of α-glucoside requires considerably larger activation barrier than that of β-glucoside. This result agrees with the experimental observation that the β-glucoside is more reactive toward levoglucosan formation than the corresponding α-glucoside. This difference in the activation barrier is interpreted in terms of the stereoelectronic effect, which stabilizes the transition state of the $S_N$icB(2) mechanism by the CT from the ring oxygen to the anomeric carbon atom. The comparison between phenyl glucosides and the corresponding phenyl 5a-carba-glucosides clearly provides theoretical evidence that the ring oxygen plays a key role to stabilize the cationic center through the stereoelectronic effect. Also, the conformation around the C1−C2 bond is eclipsed in the transition state of the α-anomer but staggered in that of the β-anomer, which is another factor for the larger reactivity of the β-anomer.

Acknowledgment. This work was financially supported by a Grant-in-Aid for JSPS Fellows (No. 20.1219), Grant-in-Aids for Specially Promoted Research No. 22000009, Grand Challenge Project from the Ministry of Education, Science, Sports, and Culture. SGI Altix4700 workstations of the Institute for Molecular Science (Okazaki, Japan) and PC cluster computers of our laboratory were used.

Supporting Information Available: Complete ref 23; geometries of important intermediates and transition states in the reactions of $\mathbf{R_\alpha}$ and $\mathbf{R_\beta}$ in gas phase and in water solution; changes in the geometries before and after the optimizations of important oxyanions of $\mathbf{R_\alpha}$ and $\mathbf{R_\beta}$; conformational changes of $\mathbf{C_\alpha}$ and $\mathbf{C_\beta}$ from $^4C_1$ to $^1C_4$; changes of the geometry and the Gibbs energy in the direct levoglucosan formation from the oxyanion of $\mathbf{R_\beta}$; NBO charges and bond orders of $\mathbf{TS_\alpha}$, $\mathbf{TS_\alpha}'$, $\mathbf{TS_{1\beta}}$, and $\mathbf{TS_{1\beta}}'$; optimized geometries of phenyl glucosides ($\mathbf{R_\alpha}$ and $\mathbf{R_\beta}$), phenyl 5a-carbaglucosides ($\mathbf{R_{C\alpha}}$ and $\mathbf{R_{C\beta}}$), and their oxyanions; E_a values evaluated with MP2 to MP4(SDQ) and DFT(B3LYP) methods; detailed discussion about the changes in the geometry in steps I-C_α and I-C_β; and Cartesian coordinates of important species. This material is available free of charge via the Internet at http://pubs.acs.org.